OPEN

Plastic and Reconstructive Surgery Advance Online Article

DOI: 10.1097/PRS.0000000000010441

Sagittal Craniosynostosis: Comparing Surgical Techniques using 3D Photogrammetry

Tareq **Abdel-Alim**[1,2]*, Melissa **Kurniawan**[3]*, Irene **Mathijssen**[3], Marjolein **Dremmen**[2], Clemens **Dirven**[1], Wiro **Niessen**[2,4], Gennady **Roshchupkin**[2,5]** & Marie-Lise **van Veelen**[1,6]**

[1] Department of Neurosurgery, Erasmus MC, University Medical Center, Rotterdam, the Netherlands

[2] Department of Radiology & Nuclear Medicine, Erasmus MC, University Medical Center, Rotterdam, the Netherlands

[3] Department of Plastic, Re constructive Surgery, and Hand Surgery, Erasmus MC, University Medical Center, Rotterdam, the Netherlands

[4] Faculty of Applied Sciences, Delft University of Technology, Delft, the Netherlands

[5] Department of Epidemiology, Erasmus MC, University Medical Center, Rotterdam, the Netherlands

[6] Pediatric Brain Center, Erasmus MC, University Medical Center, Rotterdam, the Netherlands

* These authors contributed equally to this work

** These authors have jointly supervised this work

Corresponding author: Tareq Abdel-Alim Departments of Neurosurgery and Radiology & Nuclear Medicine, Erasmus MC, University Medical Center, Rotterdam, the Netherlands E-mail: t.abdelalim@erasmusmc.nl

Financial Disclosure Statement:

Authors have no competing interests or any financial interest to declare in relation to the content of this article.

Short Running Head (no more than 40 characters in length):

Scaphocephaly surgical outcome analysis

Abstract word count: 240

Text word count: 2999

Number of references: 54

Number of tables and/or figures: 6 figures, 4 tables, 6 SDC items

Author contributions

T.A.A. and M.S.I.C. jointly conceived the study, participated in the design of the study, performed the statistical analysis, interpreted the data, and drafted the manuscript. T.A.A. additionally developed the software. M.H.G.D., W.J.N., and C.M.F.D. participated in the design of the study and revised the manuscript critically for important intellectual content. I.M.J.M., G.V.R., and M.V.V. participated in the design of the study and interpreted the data, and revised the manuscript critically for important intellectual content. G.V.R. and M.V.V. jointly supervised the work. All authors read and approved the final manuscript.

Abstract

OBJECTIVE: The aim of this study is to compare three surgical interventions to correct sagittal synostosis: frontobiparietal remodeling (FBR), extended strip craniotomy (ESC), and spring assisted correction (SAC), based on 3D photogrammetry and operation characteristics.

METHODS: All patients diagnosed with non-syndromic sagittal synostosis, born between 1991 and 2019, who underwent FBR, ESC or SAC, and had at least one postoperative 3D photogrammetry image taken during one of six follow-up moments until the age of six, were considered for this study. Operation characteristics, postoperative complications, re-interventions, and presence of intracranial hypertension were collected. To assess cranial growth, orthogonal cranial slices and 3D photocephalometric measurements were extracted automatically and evaluated from 3D photogrammetry images.

RESULTS: A total of 322 postoperative 3D images from 218 patients were included. After correcting for age and gender, no significant differences were observed in 3D photocephalometric measurements. Mean cranial shapes suggest that postoperative growth and shape gradually normalize with higher OFC and ICV values compared to normal, regardless of type of surgery. Flattening of the vertex seems to persist after surgical correction. Our cranial 3D mesh processing tool has been made publicly available as a part of this study.

CONCLUSION: Our findings suggest that until the age of six, there are no significant differences between the FBR, ESC, and SAC in their ability to correct sagittal synostosis with regard to 3D photocephalometric measurements. Therefore, efforts should be made to ensure early diagnosis so that minimally invasive surgery is still a viable treatment option.

Key Words: Craniosynostosis; Shape Analysis; Photogrammetry; Corrective surgery; Early Diagnosis; Intracranial Volume

Background

Sagittal synostosis is a congenital condition that involves premature fusion of the sagittal suture. This condition results in an elongated (anterior-posterior) and narrow (transverse) shape of the head, also known as scaphocephaly. In addition, frontal bossing or formation of an occipital bullet is frequently present.[1] Compared to other non-syndromic single suture craniosynostoses, sagittal synostosis has the highest prevalence and is estimated to affect 1 in every 2000 live births worldwide.[1–3]

Sagittal synostosis can affect the functional and aesthetic development of the child. It causes a higher risk of developing intracranial hypertension (ICH), speech and language problems, intellectual impairment, and psychological difficulties.[4–8]

Different surgical techniques have been described to correct scaphocephaly.[9,10] In the Erasmus MC the preferred surgery changed over time from Frontobiparietal remodeling (FBR) at 9-12 months of age, to extended strip craniectomy (ESC) and minimally invasive springs (SAC) before 6 months of age.[10] However, there is still no consensus on the most effective surgical technique.[11–20]

Objective measurements, such as the cephalic index (CI), occipitofrontal head circumference (OFC), and intracranial volume (ICV) are commonly used to evaluate postoperative results.[21–23] Obtaining these measurements is a cumbersome and time consuming task, involving manual measurements and traditional imaging modalities. To minimize radiation exposure and discomfort in young patients during follow-up, aesthetic outcomes of a surgical interventions are often subjectively assessed by the clinician and parents.[24] This is problematic in the pursuit of obtaining an objective consensus regarding the best treatment and timing for patients with craniosynostosis. Three-dimensional (3D) photogrammetry is a non-invasive and radiation-free imaging modality that can serve as a useful instrument in this endeavor.

A 3D photogrammetry setup is used to generate a digital 3D model of the subject's head. 3D photogrammetry is rapidly gaining popularity in clinical research and has shown to be a highly reliable, accurate, and safe instrument for reproducible craniofacial shape analysis, in both children and adults.[25]

In this study, we look at patients who had at least one postoperative 3D photogrammetry image taken up to the age of six. This age limit was chosen to balance the number of patients in the follow-up period from older and younger cohorts. It is also during those first six years that the sutures play an essential role in the development and growth of the skull, after which appositional growth takes over.[26] These images are used to analyze cranial measurements and shapes after one of three types of surgical interventions: ESC, SAC, and FBR (Figure 1). Measurements obtained from 3D photogrammetry images are referred to as 3D photocephalometrics. Additionally, operating characteristics and clinical parameters are compared based on operating time, blood loss, complications, and signs of ICH.

To stimulate transparent and reproducible research, the framework that was developed and used for mesh visualization, registration, pre-processing, and extraction of 3D photocephalometric measurements, is made publicly available as a free and open-source tool *"CraniumPy"* on Github.[27]

Patients and Methods

Patient characteristics

408 patients born between 1991 and 2019, with diagnosed non-syndromic sagittal synostosis, whom underwent FBR, ESC, or SAC in our hospital, and had at least one post-operative 3D

photogrammetry image taken before the age of six, were considered for this study. 3D images were captured using a 3dMDhead setup. No hairstyling products are allowed on the day of imaging and in the case of long hair, the hair needs to be loose and combed flat. Before acquisition, a special nylon cap is pulled tightly over the head of the patient to minimize hair-induced deformations. Images in which the head shape was camouflaged by hair were excluded during data collection.

Preoperative measurements were used to assess if preoperative differences between the groups were present.

The study protocol was approved by the Institution's medical ethical committee (MEC-2016-312) and followed the statements of the Declaration of Helsinki.

Treatment protocol

The protocol in the Erasmus MC Sophia Children's Hospital has changed over the last 15 years. Up until 2002, all patients presenting with sagittal synostosis underwent an FBR between the age of 9 and 12 months regardless of their age at presentation. However, a relatively high incidence of preoperative papilledema (9%) was observed in patients who presented early and had to wait for surgery.[28] Between 2002 and 2010 the ESC was introduced for children who presented before the age of 6 months. In 2010, we transitioned from ESC to SAC to further reduce bloodloss and extensiveness. Patients presenting after the age of 6 months undergo an FBR shortly after referral. More details about the three surgical techniques and clinical outcomes are presented in earlier studies.[10,12,29]

Postoperatively, patients have a routine follow-up involving skull radiographs, 3D photogrammetry, fundoscopy and OFC measurements at regular intervals.[30]

3D photocephalometrics and mean cranial shapes

3D images captured during at least one of six follow-up moments (FU) were included:

- **FU1**: 3 months postoperatively **and** age < 18 months
- **FU2**: 24 months of age
- **FU3**: 36 months of age
- **FU4**: 48 months of age
- **FU5**: 60 months of age
- **FU6**: 72 months of age

Measurements include:

- Maximum occipitofrontal diameter (OFD)
- Biparietal diameter
- OFC
- Orthogonal cranial slices (Figure 2)
- Approximated ICV:

A one-to-one translation from 3D photogrammetry to clinical measurements is reliable for measurements that are obtained in the same manner in clinic (OFC and CI).[25] However, volumetric measurements result in an overestimation of the intracranial volume and require a correction. This correction is based on reported correction factors in the literature and confirmed by strong linear correlation (R2=0.96) between ICV from CT and 3D photogrammetry observed in a subset of patients who had a CT scan acquired on the same day as their 3D photogrammetry image (n=25).[9,31–33]

The reference plane in our pipeline is defined by the plane going through the nasion and both tragi. The centroid of these three landmarks serves as the initial anchor point and guides the registration process (Figure, Supplemental Digital Content 1). To extract measurements, an iterative algorithm searched along slices parallel to the nasion-tragi plane. After locating the slice containing the largest OFD, an axial slice was extracted from the mesh (Figure 2). Measurements were converted to z-scores before statistical testing. The z-score describes how far each measurement is from its normocephalic, age- and gender-associated mean, expressed in standard deviation (SD). OFC measurements were converted to z-scores using Growth Analyser with reference data by Talma et al.[34] Z-scores for ICV and CI were calculated based on normal data presented by Abbott et al.[35] and Waitzman et al.[36] respectively. Complementary to the statistical comparison of measurements, mean cranial shapes were generated along three orthogonal slices.

A sagittal and coronal slice (Figure 2) perpendicular to the axial OFD slice were extracted from every mesh. For 120 sampled points on every slice, a mean and standard deviation was calculated (Figure 3a) and allowed us to generate mean cranial shapes (Figure 3b) for different techniques and age groups. A healthy age-related normal model was used as a reference.[37] Pre-processing steps are further described in the document, Supplemental Digital Content 2.

Statistical analysis

Scipy Statistics was used for statistical analysis.[38] Continuous variables were compared using the one-way ANOVA test, after the assumptions of normality (Shapiro-Wilk test) and homogeneity of variance (Levene's test) were confirmed (Table, Supplemental Digital Content 3). The Kruskal-Wallis H-test was used to compare continuous variables for which these assumptions were not true. A significance level less than 0.05 was considered significant.

Results

Patient and operation characteristics

After considering all prerequisites and exclusion criteria (Figure 4), 218 patients (58 FBR, 82 ESC, 78 SAC) with a total of 322 3D images were included in this study (Table 1). In all three groups, there were more males than females, which is in line with the epidemiology.[2] Operation characteristics and complications are presented in Table 2 and Table 3 respectively. The length of surgery was significantly different between all three surgical techniques. The FBR surgery showed more extensive blood loss, compared to ESC and SAC. Dural defects occurred in 9 patients, of which 7 in the FBR group and 2 in the SAC group.

ICH and re-interventions

15 patients (5 FBR; 8 ESC; 2 SAC) had a re-intervention due to ICH, skull defect, hematoma, or persistent scaphocephalic head shape (Table, Supplemental Digital Content 4). Patients who had a re-intervention due to ICH, underwent biparietal remodeling. Patients with skull defects underwent split skull graft and patients with a persisting scaphocephalic shape, underwent an FBR.

In 9 patients (2 FBR; 6 ESC; 1 SAC), an intracranial pressure (ICP) measurement was performed due to persistent papilledema. In 6 of those patients (1 FBR; 4 ESC; 1 SAC) ICH was confirmed. A re-intervention to reduce ICP was necessary in 5 out of the 6 patients. One patient did not have surgery, due to the disappearance of papilledema. Therefore surgery was cancelled and watchful waiting was maintained.

Re-interventions due to skull defects were performed in 4 patients who were treated with FBR and 3 patients with ESC. A single patient treated with ESC required a re-intervention due to a postoperative hematoma.

3D photocephalometrics and mean cranial shapes

Preoperative measurements from skull radiographs (CI) and manual measurements (OFC) were used to determine a preoperative baseline. We observed no significant differences in preoperative CI and OFC between the three groups after correcting for age and gender (Table, Supplemental Digital Content 5). Preoperative ICV measurements were not available. However, the OFC has shown to be a good proxy for ICV.[39] This was verified using postoperative ICV and OFC measurements, which showed a strong correlation (R_2=0.89). We therefore assumed a similar non-significant difference in preoperative ICV between the three groups.

Mean postoperative cranial shapes with respect to normocephalic head shapes from a statistical shape model (SSM) are presented in Figure 5.[37] Extracted OFC, CI, and ICV values are presented in Table 4 and plotted in Figure 6. Statistical testing showed no significant differences in z-scores between the three groups with the exception of ICV in the follow-up group at 72 months (Table 4). However, post-hoc tests with a Bonferroni correction to correct for multiple comparisons did not show significant pair wise differences in ICV.

Early on, the cranial shapes in the axial and sagittal plane (Figure 5) show that scaphocephalic features such as frontal bossing and occipital bullet persist up until the age of 24 months, regardless of the operating technique. The data shows that at 24 months, the mean OFC and ICV are 1SD above normal with a CI of -0.5SD. Over time, the CI normalizes as shown in Figure 5 with a mean CI value of -0.03SD at 36 months, -0.12SD at 48 months, and -0.27SD at 60 and 72 months. At 36, 48, 60, and 72 months respectively, increased mean OFC (+0.58SD, +0.69SD, +0.64SD, +0.85SD) and ICV (+1.05SD, +1.30SD, +1.37SD, +1.68SD) values are observed compared to normal.

Flattening of the vertex can be observed in the sagittal and coronal planes in FU 5 and 6 (Figure 5), causing an anterior displacement of the position of maximum vertex height. The ESC FU6 group shows the lowest vertex with respect to the other two groups. The width of the skull is not evidently different from the normal population.

Discussion

This study is one of the largest studies in the evaluation of three surgical techniques until the age of six based on both 3D photogrammetry and operating characteristics.

Postoperative outcomes

Many studies have compared surgical outcomes to determine the differences in surgical techniques based on CI, OFC, and ICV. In a review by Bonfield et al. (2014), it was reported that cranial vault remodeling (CVR) and Endoscopic-Assisted Craniectomy (EAC) led to the largest improvement in CI compared to other surgical techniques, including SAC and ESC. This larger effect is possibly explained by a lower preoperative CI in the CVR and EAC groups, according to the authors.[18] Differences in OFC between surgeries vary within the literature. De Praeter et al. (2019) showed a larger increase in OFC for the CVR compared to ESC in a small study.[19] However, we have not found significant differences in postoperative CI and OFC between the surgeries (Table 4), which is in line with the majority of comparable studies.[17,20,40–42]

Fischer et al. and Mertens et al. both indicated no differences in ICV measures after SAC or ESC compared to pi-plasty surgery.[43,44] Contrary, Arab et al. concluded that extensive cranioplasties resulted in a smaller ICV, whereas SAC and ESC combined did not show these results.[45] The problem of a smaller ICV is that it might be related to the development of ICH, an important complication seen in patients with craniosynostosis.[46–48] Our results showed no differences in z-scores of postoperative ICV in the first 5 follow-up groups. Relatively large differences in ICV were observed in the final follow-up group at the age of 72 months (Table 4). Pairwise post-hoc tests were unable to detect significant differences, which may be caused by a low statistical power. These differences may however be clinically relevant with regard to the long-term effects of the surgical techniques. Do for example these smaller ICVs in the ESC group relate to an increase in hypertension or does the relatively large ICV in the FBR group result in other complications later in life? To obtain conclusive answers to these questions, larger studies and collaborations are required.

When we look at the postoperative outcomes in comparison to the normative population, we clearly see a normalization of the CI in all three groups, while both OFC and ICV values were consistently higher than normal for their age. We hypothesize that this is due to the fact that the three techniques focus on harmonization of craniofacial proportions, attaining a near normal CI by widening rather than shortening of the head when correcting the scaphocephalic shape. With an above average head depth inherent to this condition, this "harmonization" inevitably leads to an increased OFC and ICV value compared to normal. The persistence of larger than normal OFC and ICV values may suggest that normative growth potential is not impaired by these interventions. Sgouros et al. (1999) reported similar results in a study on postoperative ICV development in craniosynostosis and observed that these children followed a growth curve parallel to that of healthy children with a considerably higher volume.[49] A significantly larger than normal OFC and ICV were also reported by Toma et al. (2010) after total vault remodelling.[50]

The generated mean cranial shapes (Figure 5) show that all three techniques generally correct the distinctive scaphocephalic features, such as frontal bossing and occipital bulging. The observable differences in mean shape between the three operating groups in the first two follow-up moments, could be explained by the significant difference in mean age at surgery (Table 2) instead of an inherent effect of a particular operating technique. Longitudinal visualizations of mean shapes for every operating technique confirm this discrepancy between the first and second follow-up group (Figure, Supplemental Digital Content 6). Frontal and occipital regions correct over time, irrespective of the inclusion of the forehead or occiput in the remodelling. Flattening of the vertex seems to persist after surgical correction (Figure 5; FU 5 and 6). Correcting the position of the vertex remains a challenge and may guide future modifications of surgical techniques.

The mean shape visualizations corroborate our statistical results that postoperative differences between operating techniques are limited and show us that more comprehensive parameters are required to evaluate the cranial morphology and all its intricacies in three dimensions.

<u>Importance of an early diagnosis and the potential of 3D photogrammetry</u>

Our findings show that FBR is associated with a longer mean surgery time, an increased risk of dural defects, and higher blood loss compared to ESC and SAC (Table 2). This result is in line with other reports and favors early minimal intervention above late extensive surgery. Since the age at presentation is the decisive factor for the type of surgery a patient receives, it is important to emphasize the importance of an early diagnosis. In addition to increasing awareness about the early signs of craniosynostosis, the development of novel diagnostic tools may be helpful early on. When craniosynostosis is suspected, a patient always has to be referred to a craniofacial center for further examination and diagnosis.

Novel machine learning methods for classifying and quantifying different types and severities of craniosynostoses based on 3D photogrammetry data have already shown good results.[51,52] Next steps may involve the use of deep learning methods, such as autoencoders based on mesh convolution operators.[53,54]

Study limitations

Data was not evenly distributed within the FU groups. It is therefore important to consider the number of samples used to generate the mean shapes, as well as differences between age groups when interpreting the results.

We demonstrated that 3D photogrammetry can be used for rapid automatic extraction of measurements, without the need for labor-intensive measurements and invasive imaging modalities. However, the complexity of cranial development makes finding a stationary reference point for craniofacial analysis challenging, in particular when landmarks are limited to distinct features on the subject's surface. Our reference point, based on the center of mass, is easy to reproduce and provides relevant information about the skull shape development. This reference point will likely be less suitable for the detection of anisotropic growth effects (e.g. excessive anterior growth), since these effects will be averaged out when using the center of mass.

Conclusion

No statistically significant differences in CI, OFC, and ICV were observed between the surgical interventions, while FBR has a longer mean surgery time and shows a larger number of dural defects and higher blood loss than ESC and SAC. Since age at presentation is the main determinant on the basis of which minimally invasive surgery can be considered, early diagnosis is important. 3D photogrammetry offers the opportunity to acquire high-dimensional, longitudinal data for retrospective analysis, and can be a promising way forward in the early detection of craniofacial dysmorphologies and to enhance personalized treatment. As a part of this study, our 3D image processing tool has been made publicly available for pre-processing of 3D meshes and extraction of 3D photocephalometric measurements in a quick, accessible and reproducible manner.

Acknowledgements

The authors would like to thank Nicole Erler, biostatistician in the Erasmus MC, who was readily available for questions and discussions regarding the statistical analysis of this study.

Bibliography

1. Governale LS. Craniosynostosis. Pediatr Neurol. 2015;53(5):394–401.
2. Cornelissen M, Ottelander B den, Rizopoulos D, van der Hulst R, Mink van der Molen A, van der Horst C, et al. Increase of prevalence of craniosynostosis. J Cranio-Maxillofacial Surg [Internet]. 2016;44(9):1273–9. Available from: http://dx.doi.org/10.1016/j.jcms.2016.07.007
3. Fearon JA. Evidence-based medicine: Craniosynostosis. Plast Reconstr Surg [Internet]. 2014;133(5):1261–75. Available from: https://pubmed.ncbi.nlm.nih.gov/24776557/
4. Kapp-Simon KA, Speltz ML, Cunningham ML, Patel PK, Tomita T. Neurodevelopment of children with single suture craniosynostosis: A review [Internet]. Vol. 23, Child's Nervous System. Childs Nerv Syst; 2007. p. 269–81. Available from: https://pubmed.ncbi.nlm.nih.gov/17186250/
5. Kapp-Simon KA, Collett BR, Barr-Schinzel MA, Cradock MM, Buono LA, Pietila KE, et al. Behavioral adjustment of toddler and preschool-aged children with single-suture craniosynostosis. Plast Reconstr Surg [Internet]. 2012 Sep;130(3):635–47. Available from: https://pubmed.ncbi.nlm.nih.gov/22929249/
6. Cloonan YK, Collett B, Speltz ML, Anderka M, Werler MM. Psychosocial outcomes in children with and without non-syndromic craniosynostosis: Findings from two studies. Cleft Palate-Craniofacial J [Internet]. 2013 Jul;50(4):406–13. Available from: https://pubmed.ncbi.nlm.nih.gov/22315944/
7. Arnaud E, Renier D, Marchac D. Prognosis for mental function in scaphocephaly. J Neurosurg [Internet]. 1995;83(3):476–9. Available from: https://pubmed.ncbi.nlm.nih.gov/7666225/

8. Alperovich M, Runyan CM, Gabrick KS, Wu RT, Morgan C, Park SE, et al. Long-Term Neurocognitive Outcomes of Spring-Assisted Surgery versus Cranial Vault Remodeling for Sagittal Synostosis. Plast Reconstr Surg [Internet]. 2021 [cited 2021 Nov 19];147(3):661–71. Available from: https://pubmed.ncbi.nlm.nih.gov/33620934/

9. van Veelen MLC, Jippes M, Carolina JCA, de Rooi J, Dirven CMF, van Adrichem LNA, et al. Volume measurements on three-dimensional photogrammetry after extended strip versus total cranial remodeling for sagittal synostosis: A comparative cohort study. J Cranio-Maxillofacial Surg [Internet]. 2016;44(10):1713–8. Available from: http://dx.doi.org/10.1016/j.jcms.2016.07.029

10. Van Veelen MLC, Mathijssen IMJ. Spring-assisted correction of sagittal suture synostosis. Child's Nerv Syst. 2012;28(9):1347–51.

11. Mandela R, Bellew M, Chumas P, Nash H. Impact of surgery timing for craniosynostosis on neurodevelopmental outcomes: A systematic review. J Neurosurg Pediatr. 2019 Apr;23(4):442–54.

12. van Veelen ML, Mihajlovic D, Dammers R, Lingsma H, van Adrichem LN, Mathijssen IM. Frontobiparietal remodeling with or without a widening bridge for sagittal synostosis: comparison of 2 cohorts for aesthetic and functional outcome. J Neurosurg Pediatr [Internet]. 2015;16(1):86–93. Available from: https://ovidsp.ovid.com/ovidweb.cgi?T=JS&CSC=Y&NEWS=N&PAGE=fulltext&D=med12&AN=25910033

13. Brandel MG, Dalle Ore CL, Reid CM, Zhu W, Lance S, Meltzer H, et al. Distraction osteogenesis for unicoronal craniosynostosis: Rotational flap technique and case series. Plast Reconstr Surg. 2018;142(6):904E-908E.

14. Linz C, Meyer-Marcotty P, Böhm H, Müller-Richter U, Jager B, Hartmann S, et al. 3D stereophotogrammetric analysis of operative effects after broad median craniectomy in premature sagittal craniosynostosis. Child's Nerv Syst. 2014 Feb;30(2):313–8.
15. Safi AF, Kreppel M, Grandoch A, Kauke M, Nickenig HJ, Zöller J. Clinical Evaluation of Standardized Fronto-Orbital Advancement for Correction of Isolated Trigonocephaly. J Craniofac Surg. 2018 Jan;29(1):72–5.
16. Borghi A, Rodriguez-Florez N, Rodgers W, James G, Hayward R, Dunaway D, et al. Spring assisted cranioplasty: A patient specific computational model. MED ENG PHYS [Internet]. 2018;53:58–65. Available from: http://www.embase.com/search/results?subaction=viewrecord&from=export&id=L620258152
17. Lepard J, Hassan S, Mooney J, Arynchyna A, McClugage SG, Myers RP, et al. Comparison of aesthetic outcomes between open and endoscopically treated sagittal craniosynostosis. J Neurosurg Pediatr [Internet]. 2021 Jul 30 [cited 2021 Nov 15];28(4):432–8. Available from: https://thejns.org/pediatrics/view/journals/j-neurosurg-pediatr/28/4/article-p432.xml
18. Bonfield CM, Lee PS, Adamo MA, Pollack IF. Surgical treatment of sagittal synostosis by extended strip craniectomy: Cranial index, nasofrontal angle, reoperation rate, and a review of the literature. J Cranio-Maxillofacial Surg [Internet]. 2014 Oct 1 [cited 2021 Nov 18];42(7):1095–101. Available from: https://pubmed.ncbi.nlm.nih.gov/24530081/
19. De Praeter M, Nadjmi N, Reith FCM, Vercruysse H, Menovsky T. Is There an Advantage to Minimizing Surgery in Scaphocephaly? A Study on Extended Strip

Craniotomy Versus Extensive Cranial Vault Remodeling. J Craniofac Surg [Internet]. 2019 Sep 1;30(6):1714–8. Available from: https://pubmed.ncbi.nlm.nih.gov/31022147/

20. Runyan CM, Gabrick KS, Park JG, Massary D, Hemal K, Owens ES, et al. Long-Term Outcomes of Spring-Assisted Surgery for Sagittal Craniosynostosis. Plast Reconstr Surg [Internet]. 2020 [cited 2021 Nov 17];146(4):833–41. Available from: https://pubmed.ncbi.nlm.nih.gov/32590513/

21. Leikola J, Koljonen V, Heliövaara A, Hukki J, Koivikko M. Cephalic index correlates poorly with intracranial volume in non-syndromic scaphocephalic patients. Child's Nerv Syst [Internet]. 2014 Jun 26;30(12):2097–102. Available from: https://link.springer.com/article/10.1007/s00381-014-2456-x

22. Heller JB, Heller MM, Knoll B, Gabbay JS, Duncan C, Persing JA. Intracranial volume and cephalic index outcomes for total calvarial reconstruction among nonsyndromic sagittal synostosis patients. Plast Reconstr Surg [Internet]. 2008 Jan;121(1):187–95. Available from: https://pubmed.ncbi.nlm.nih.gov/18176220/

23. Bergquist CS, Nauta AC, Selden NR, Kuang AA. Age at the Time of Surgery and Maintenance of Head Size in Nonsyndromic Sagittal Craniosynostosis. Plast Reconstr Surg [Internet]. 2016 May 1;137(5):1557–65. Available from: https://pubmed.ncbi.nlm.nih.gov/27119928/

24. Bendon CL, Johnson HP, Judge AD, Wall SA, Johnson D. The aesthetic outcome of surgical correction for sagittal synostosis can be reliably scored by a novel method of preoperative and postoperative visual assessment. Plast Reconstr Surg [Internet]. 2014;134(5):775e-786e. Available from: https://pubmed.ncbi.nlm.nih.gov/25347653/

25. Abdel-Alim T, Iping R, Wolvius EB, Mathijssen IMJ, Dirven CMF, Niessen WJ, et al.

Three-Dimensional Stereophotogrammetry in the Evaluation of Craniosynostosis: Current and Potential Use Cases. J Craniofac Surg [Internet]. 2021 May;32(3):956–63. Available from: https://journals.lww.com/jcraniofacialsurgery/Fulltext/2021/05000/Three_Dimensional_Stereophotogrammetry_in_the.35.aspx

26. Mathijssen IMJ. Guideline for care of patients with the diagnoses of craniosynostosis: working group on craniosynostosis. The Journal of craniofacial surgery. ncbi.nlm.nih.gov; 2015.

27. Abdel-Alim T. CraniumPy [Internet]. 2021. Available from: https://github.com/T-AbdelAlim/CraniumPy

28. van Veelen MLC, Kamst N, Touw C, Mauff K, Versnel S, Dammers R, et al. Minimally Invasive, Spring-Assisted Correction of Sagittal Suture Synostosis: Technique, Outcome, and Complications in 83 Cases. PLAST RECONSTR SURG [Internet]. 2018;141(2):423–33. Available from: http://www.embase.com/search/results?subaction=viewrecord&from=export&id=L622912421

29. Van Veelen MLC, Eelkman Rooda OHJ, De Jong T, Dammers R, Van Adrichem LNA, Mathijssen IMJ. Results of early surgery for sagittal suture synostosis: Long-term follow-up and the occurrence of raised intracranial pressure. Child's Nerv Syst [Internet]. 2013 Jun 20;29(6):997–1005. Available from: https://link.springer.com/article/10.1007/s00381-013-2024-9

30. Mathijssen IMJ. Updated Guideline on Treatment and Management of Craniosynostosis. J Craniofac Surg [Internet]. 2021 Jan 1 [cited 2021 Nov

23];32(1):371–450. Available from: https://journals.lww.com/jcraniofacialsurgery/Fulltext/2021/02000/Updated_Guideline_on_Treatment_and_Management_of.93.aspx

31. McKay DR, Davidge KM, Williams SK, Ellis LA, Chong DK, Teixeira RP, et al. Measuring cranial vault volume with three-dimensional photography: A method of measurement comparable to the gold standard. J Craniofac Surg. 2010;21(5):1419–22.

32. Tu L, Porras AR, Enquobahrie A, Graham GC, Tsering, M.s. D, Horvath S, et al. Automated Measurement of Intracranial Volume Using Three-Dimensional Photography. Plast Reconstr Surg [Internet]. 2020 [cited 2022 Apr 19];146(3):314E-323E. Available from: https://pubmed.ncbi.nlm.nih.gov/32459727/

33. Tu L, Porras AR, Ensel S, Tsering D, Paniagua B, Enquobahrie A, et al. Intracranial Volume Quantification from 3D Photography. In: Lecture Notes in Computer Science (including subseries Lecture Notes in Artificial Intelligence and Lecture Notes in Bioinformatics) [Internet]. Comput Assist Robot Endosc Clin Image Based Proced (2017); 2017 [cited 2022 Apr 19]. p. 116–23. Available from: https://pubmed.ncbi.nlm.nih.gov/29167840/

34. Talma H, Schonbeck Y, Bakker B, Hirasing RA, van Buuren S. Groeidiagrammen 2010: Handleiding bij het meten en wegen van kinderen en het invullen van groeidiagrammen [Internet]. TNO; 2010 [cited 2021 Nov 20]. (in Dutch). Available from: https://repository.tno.nl/islandora/object/uuid%3A5460503b-1519-4db0-8309-d8a63ecca01e

35. Abbott AH, Netherway DJ, Niemann DB, Clark B, Yamamoto M, Cole J, et al. CT-determined intracranial volume for a normal population. J Craniofac Surg [Internet].

2000 [cited 2021 Nov 17];11(3):211–23. Available from: https://pubmed.ncbi.nlm.nih.gov/11314299/

36. Waitzman AA, Posnick JC, Armstrong DC, Pron GE. Craniofacial Skeletal Measurements Based on Computed Tomography: Part II. Normal Values and Growth Trends. Cleft Palate-Craniofacial J [Internet]. 1992 Dec 15 [cited 2021 Dec 8];29(2):118–28. Available from: https://journals.sagepub.com/doi/10.1597/1545-1569_1992_029_0118_csmboc_2.3.co_2

37. T. Huysmans, L. Goto, J. Molenbroek RG. DINED Mannequin. Tijdschr voor Hum Factors. 2020;45(1):4--7.

38. Virtanen P, Gommers R, Oliphant TE, Haberland M, Reddy T, Cournapeau D, et al. SciPy 1.0: fundamental algorithms for scientific computing in Python. Nat Methods [Internet]. 2020 Feb 3 [cited 2022 May 20];17(3):261–72. Available from: https://www.nature.com/articles/s41592-019-0686-2

39. Hashmi A, Cahill GL, Zaldana M, Davis G, Cronin BJ, Brandel MG, et al. Can Head Circumference Be Used as a Proxy for Intracranial Volume in Patients With Craniosynostosis? Ann Plast Surg [Internet]. 2019 May 1 [cited 2021 Nov 18];82(5S Suppl 4):S295–300. Available from: https://pubmed.ncbi.nlm.nih.gov/30973835/

40. Gerety PA, Basta MN, Fischer JP, Taylor JA. Operative management of nonsyndromic sagittal synostosis: A head-to-head meta-analysis of outcomes comparing 3 techniques. J Craniofac Surg [Internet]. 2015 Jun 1;26(4):1251–7. Available from: https://pubmed.ncbi.nlm.nih.gov/26080168/

41. Le MB, Patel K, Skolnick G, Naidoo S, Smyth M, Kane A, et al. Assessing long-term outcomes of open and endoscopic sagittal synostosis reconstruction using three-

dimensional photography. J Craniofac Surg [Internet]. 2014 [cited 2021 Nov 18];25(2):573–6. Available from: https://pubmed.ncbi.nlm.nih.gov/24577302/

42. Thomas GPL, Johnson D, Byren JC, Jayamohan J, Magdum SA, Richards PG, et al. Long-term morphological outcomes in nonsyndromic sagittal craniosynostosis: A comparison of 2 techniques. J Craniofac Surg [Internet]. 2015 Jan 21 [cited 2021 Nov 18];26(1):19–25. Available from: https://pubmed.ncbi.nlm.nih.gov/25569384/

43. Fischer S, Maltese G, Tarnow P, Wikberg E, Bernhardt P, Kolby L. Comparison of intracranial volume and cephalic index after correction of sagittal synostosis with spring-assisted surgery or pi-plasty. In: Journal of Craniofacial Surgery [Internet]. J Craniofac Surg; 2016 [cited 2021 Nov 18]. p. 410–3. Available from: https://pubmed.ncbi.nlm.nih.gov/26963298/

44. Mertens C, Wessel E, Berger M, Ristow O, Hoffmann J, Kansy K, et al. The value of three-dimensional photogrammetry in isolated sagittal synostosis: Impact of age and surgical technique on intracranial volume and cephalic index─a retrospective cohort study. J Cranio-Maxillofacial Surg [Internet]. 2017 Dec 1 [cited 2021 Nov 18];45(12):2010–6. Available from: https://pubmed.ncbi.nlm.nih.gov/29066040/

45. Arab K, Fischer S, Bahtti-Softeland M, Maltese G, Kolby L, Tarnow P. Comparison between two different isolated craniosynostosis techniques: Does it affect cranial bone growth? J Craniofac Surg [Internet]. 2016 Jul 1 [cited 2021 Nov 18];27(5):e454–7. Available from: https://pubmed.ncbi.nlm.nih.gov/27315320/

46. Thomas GPL, Johnson D, Byren JC, Judge AD, Jayamohan J, Magdum SA, et al. The incidence of raised intracranial pressure in nonsyndromic sagittal craniosynostosis following primary surgery. J Neurosurg Pediatr [Internet]. 2015 Apr 1;15(4):350–60.

Available from: https://pubmed.ncbi.nlm.nih.gov/25559921/

47. Gault DT, Renier D, Marchac D, Jones BM. Intracranial pressure and intracranial volume in children with craniosynostosis. Plast Reconstr Surg. 1992;90(3):377–81.

48. Fok H, Jones BM, Gault DG, Andar U, Hayward R. Relationship between intracranial pressure and intracranial volume in craniosynostosis. Br J Plast Surg. 1992 Jan;45(5):394–7.

49. Sgouros S, Hockley AD, Goldin JH, Wake MJC, Natarajan K. Intracranial volume change in craniosynostosis. J Neurosurg [Internet]. 1999 [cited 2022 Apr 20];91(4):617–25. Available from: https://pubmed.ncbi.nlm.nih.gov/10507384/

50. Toma R, Greensmith AL, Meara JG, Da Costa AC, Ellis LA, Willams SK, et al. Quantitative morphometric outcomes following the melbourne method of total vault remodeling for scaphocephaly. In: Journal of Craniofacial Surgery [Internet]. J Craniofac Surg; 2010 [cited 2022 Apr 20]. p. 637–43. Available from: https://pubmed.ncbi.nlm.nih.gov/20485021/

51. de Jong G, Bijlsma E, Meulstee J, Wennen M, van Lindert E, Maal T, et al. Combining deep learning with 3D stereophotogrammetry for craniosynostosis diagnosis. Sci Rep [Internet]. 2020 Sep 18 [cited 2021 Nov 19];10(1):1–6. Available from: https://www.nature.com/articles/s41598-020-72143-y

52. Cho MJ, Hallac RR, Effendi M, Seaward JR, Kane AA. Comparison of an unsupervised machine learning algorithm and surgeon diagnosis in the clinical differentiation of metopic craniosynostosis and benign metopic ridge. Sci Rep. 2018;8(1).

53. Gong S, Chen L, Bronstein M, Zafeiriou S. SpiralNet++: A fast and highly efficient

mesh convolution operator. In: Proceedings - 2019 International Conference on Computer Vision Workshop, ICCVW 2019 [Internet]. Institute of Electrical and Electronics Engineers Inc.; 2019 [cited 2021 Nov 26]. p. 4141–8. Available from: https://ui.adsabs.harvard.edu/abs/2019arXiv191105856G/abstract

54. Mahdi SS, Nauwelaers N, Joris P, Bouritsas G, Gong S, Walsh S, et al. Matching 3D Facial Shape to Demographic Properties by Geometric Metric Learning: A Part-Based Approach. IEEE Trans Biometrics, Behav Identity Sci. 2021 Jun 29;1–1.

Call outs and legends

Main text

Figure 1: Surgical techniques to correct sagittal synostosis: Extended Strip Craniotomy (ESC), Spring Assisted Correction (SAC), Frontobiparietal Remodelling (FBR)

Figure 2: Extracted orthogonal slices from a 3D image

Figure 3: (a) Overlayed axial slices extracted from different 3D images. (b) Generated mean shape and corresponding SDs

Figure 4: Flow chart of study inclusion criteria

Figure 5: Mean postoperative cranial shapes from six follow-up groups w.r.t. their age specific normocephalic shape

Figure 6: Photocephalometric measurements (z-scores) from every operating group over time expressed in SDs. (above) Head circumference. (center) Cephalic index. (below) Intracranial volume

Table 1: Patient characteristics

Table 2: Operation characteristics

Table 3: Complication frequency

Table 4: Postoperative photocephalometric measurements

Supplemental Digital Content

Figure, Supplemental Digital Content 1: (left) Three selected landmarks (nasion, left tragus, right tragus) and their corresponding centroid. (center) Transformation from source to template involving a translation of the center of mass and three rotations (x,y,z) around the orthogonal unit vectors. (right) Center of mass translation based on the extracted axial slice containing the largest head circumference

Document, Supplemental Digital Content 2: Pre-processing of 3D photogrammetry images

Table, Supplemental Digital Content 3: Statistical test selection for continuous variables

Table, Supplemental Digital Content 4: ICH and re-interventions

Table, Supplemental Digital Content 5: Preoperative baseline evaluation

Figure, Supplemental Digital Content 6: Mean postoperative cranial shape development over time for every operating group.

	FBR	ESC	SAC	Overall
No. of patients	58	82	78	218
Female *(%)*	12 (20.7%)	10 (12.2%)	13 (16.7%)	35 (16.1%)
Male *(%)*	46 (79.3%)	73 (87.8%)	65 (83.3%)	184 (83.9%)
No. of 3D images	82	128	112	322
Age at 3D image follow-up *(Median [IQR])*				
3 month postop (FU1)	15.09 [13.75-15.82]	8.48 [7.99-9.18]	9.40 [8.65-10.09]	
No. of 3D images	18	48	13	
24 months (FU2)	23.92 [23.19-24.43]	24.33 [20.73-27.35]	24.49 [23.86-25.40]	
No. of 3D images	16	26	26	
36 months (FU3)	37.33 [37.17-39.08]	33.99 [31.28-36.31]	36.61 [35.88-37.50]	
No. of 3D images	8	11	34	
48 months (FU4)	47.90 [47.47-49.84]	47.44 [46.42-49.12]	49.97 [48.00-50.20]	
No. of 3D images	20	21	17	
60 months (FU5)	59.15 [58.96-60.01]	60.99 [59.53-62.18]	61.22 [60.56-61.94]	
No. of 3D images	3	4	9	
72 months (FU6)	72.26 [71.84-73.97]	72.59 [71.15-75.08]	73.64 [72.20-75.45]	
No. of 3D images	17	18	13	
FBR: frontobiparietal remodelling ESC: extended strip craniotomy SAC: spring assisted correction				

Table 1. Patient characteristics

	No. of patients evaluated	FBR n=58	ESC n=82	SAC n=78	Overall n=218	p-value
Operation characteristics						
Age at surgery (months) Median [IQR]	218	11.55 [10.51-12.64]	4.90 [4.31-5.5]	5.75 [5.41-6.00]	5.77 [5.1-9.13]	<0.001[1]
Surgery time (minutes) Median [IQR]	218	296.5 [269.25-329]	230 [205.5-258]	198.5 [174-222.5]	234 [198-275]	<0.001[1]
Blood loss (ml) Median [IQR]	207 57 FBR 78 ESC 72 SAC	600 [415-1000]	150 [100-300]	70 [43.8-121.3]	153.5 [80-400]	<0.001[1]

1. **Kruskal-Wallis rank sum test (post-hoc Conover's test)**

Table 2. Operation characteristics

	No. of patients evaluated	FBR (n=58)	ESC (n=82)	SAC (n=78)	Overall
Disturbed wound healing	218	1 (1.7%)	0 (0.0%)	1 (1.3%)	2 (0.9%)
Dural tear	218	7 (12.1%)	0 (0.0%)	2 (2.6%)	9 (4.1%)
Infection	218	3 (5.2%)	3 (3.7%)	3 (3.8%)	9 (4.1%)
Hematoma	218	0 (0.0%)	1 (1.2%)	0 (0.0%)	1 (0.5%)

Table 3. Complication frequency (%)

Surgery Follow-up group (no. 3D)	**OFC**		**CI**		**ICV**	
	(cm) mean (SD)	**z-score** mean (SD) median [IQR]	**(%)** mean (SD)	**z-score** mean (SD) median [IQR]	**(cc)** mean (SD)	**z-score** mean (SD) median [IQR]
FU1: 3 months postoperatively (no. 3D images: 79)						
Total (79)	*48.29 (1.83)*	*1.49 (1.09)* *1.42 [0.67-2.19]*	*75.32 (3.57)*	*-0.24 (0.41)* *-0.22 [-0.5-0.05]*	*1204 (138)*	*1.97 (1.35)* *1.80 [0.99-2.88]*
FBR (18)	50.26 (1.50)	1.77 (1.05) *1.46 [0.96-2.78]*	74.47 (3.87)	-0.31 (0.44) *-0.40 [-0.61- -0.02]*	1360 (94)	2.01 (1.10) *2.01 [1.27-2.67]*
ESC (48)	47.58 (1.56)	1.35 (1.16) *1.22 [0.50-2.02]*	75.53 (3.47)	-0.19 (0.38) *-0.12 [-0.43-0.05]*	1138 (113)	1.76 (1.45) *1.50 [0.75-2.38]*
SAC (13)	48.18 (1.17)	1.63 (0.83) *1.44 [1.33-1.70]*	75.75 (3.59)	-0.35 (0.45) *-0.41 [-0.49- -0.03]*	1235 (84)	2.70 (1.08) *2.91 [2.06-3.09]*
p-value		p=0.289[1]		p=0.345[2]		p=0.080[2]
FU2: 24 months of age (no. 3D images: 68)						
Total (68)	*50.72 (1.67)*	*0.99 (1.03)* 1.03 [0.25-1.58]	*73.50 (3.60)*	*-0.48 (0.39)* -0.45 [-0.79 - -0.25]	*1408 (122)*	*1.08 (1.09)* *1.13 [0.25-1.69]*
FBR (16)	51.32 (1.92)	1.43 (1.08) *1.29 [0.47-2.0]*	72.35 (2.91)	-0.62 (0.31) *-0.58 [-0.79- -0.36]*	1463 (140)	1.62 (1.07) *1.53 [1.08-2.16]*
ESC (26)	50.97 (1.44)	1.13 (0.94) *0.87 [0.38-1.71]*	73.89 (3.55)	-0.42 (0.38) *-0.40 [-0.76- -0.05]*	1394 (104)	0.96 (0.98) *0.82 [0.20-1.37]*
SAC (26)	50.11 (1.59)	0.59 (0.96) *0.82 [-0.05-1.26]*	73.81 (4.00)	-0.45 (0.42) *-0.45 [-0.86- -0.13]*	1388 (122)	0.86 (1.13) *1.12 [0.20-1.48]*
p-value		p=0.055[1]		p=0.239[2]		P=0.066[1]
FU3: 36 months of age (no. 3D images: 53)						
Total (53)	*51.32 (1.78)*	*0.58 (1.01)* *0.8 [0.06-1.27]*	*74.38 (3.78)*	*-0.03 (0.52)* *0.01 [-0.32-0.29]*	*1475 (138)*	*1.05 (1.16)* *1.0 [0.33-1.64]*
FBR (8)	51.05 (1.51)	0.41 (0.80) *0.41 [-0.02-0.76]*	76.24 (5.03)	0.23 (0.68) *0.16 [0.06-0.42]*	1442 (95)	0.85 (0.63) *0.89 [0.50-1.01]*
ESC (11)	51.05 (1.74)	0.55 (1.18) *0.50 [-0.32-1.67]*	75.08 (3.66)	-0.01 (0.51) *0.01 [-0.31-0.14]*	1435 (120)	0.74 (1.16) *0.58 [0.12-1.52]*
SAC (34)	51.48 (1.87)	0.63 (1.02) *0.88 [0.40-1.23]*	73.72 (3.41)	-0.11 (0.48) *-0.08 [-0.40-0.26]*	1495 (151)	1.19 (1.25) *1.38 [0.67-2.15]*
p-value		p=0.678[1]		p=0.252[2]		p=0.478[2]
FU4: 48 months of age (no. 3D images: 58)						
Total (58)	*52.25 (1.73)*	*0.69 (1.02)* *0.38 [-0.01-1.42]*	*73.82 (4.44)*	*-0.12 (0.61)* -0.06 [-0.48-0.25]	*1544 (136)*	*1.30 (1.17)* 1.16 [0.51-2.0]
FBR (20)	52.24 (1.70)	0.67 (1.01) *0.38 [0.03-1.17]*	73.58 (3.80)	-0.14 (0.53) *-0.02 [-0.50-0.19]*	1544 (136)	1.29 (1.22) *0.92 [0.49-1.76]*
ESC (21)	52.50 (1.74)	0.85 (1.07) *0.39 [0.03-1.68]*	74.04 (5.42)	-0.09 (0.75) *-0.01 [-0.55-0.28]*	1552 (107)	1.38 (0.94) *1.23 [0.83-1.87]*
SAC (17)	51.96 (1.83)	0.51 (1.02) *0.37 [-0.15-1.25]*	73.83 (4.02)	-0.12 (0.54) *-0.31 [-0.47-0.37]*	1536 (172)	1.23 (1.39) *1.18 [0.29-2.08]*
p-value		p=0.596[2]		p=0.963[2]		p=0.771[1]
FU5: 60 months of age (no. 3D images: 16)						
Total (16)	*52.33 (2.21)*	*0.64 (1.39)* *0.62 [0.03-1.22]*	*73.03 (3.67)*	*-0.27 (0.44)* *-0.29 [-0.51-0.0]*	*1551 (149)*	*1.37 (1.46)* *1.30 [0.71-2.12]*

FBR (3) **ESC (4)** **SAC (9)**	52.43 (1.63) 53.10 (1.34) 51.97 (2.71)	0.96 (1.23) *0.70 [0.29-1.50]* 0.94 (0.82) *0.71 [0.49-1.15]* 0.40 (1.68) *0.37 [-0.42-1.10]*	72.8 (2.44) 73.9 (2.48) 72.71 (4.57)	-0.28 (0.30) *-0.14 [-0.38- -0.11]* -0.17 (0.30) *-0.17 [-0.37-0.03]* -0.32 (0.55) *-0.37 [-0.54-0.06]*	1558 (42) 1578 (93) 1536 (193)	2.02 (0.84) *2.07 [1.61-2.45]* 1.27 (0.81) *1.19 [0.74-1.72]* 1.20 (1.83) *1.15 [-0.31-1.77]*
p-value		p=0.759[2]		p=0.871[2]		p=0.723[2]
FU6: 72 months of age (no. 3D image: 48)						
Total (48)	*53.09 (1.68)*	*0.85 (0.98)* *0.74 [0.38-1.34]*	*74.11 (3.53)*	*-0.27 (0.49)* *-0.29 [-0.73-0.12]*	*1618 (141)*	*1.68 (1.17)* *1.78 [0.71-2.41]*
FBR (17) **ESC (18)** **SAC (13)**	53.54 (1.90) 52.52 (1.61) 53.30 (1.34)	1.15 (1.07) *1.05 [0.52-1.93]* 0.54 (0.98) *0.51 [0.19-0.94]* 0.90 (0.78) *0.85 [0.32-1.20]*	73.78 (3.48) 75.45 (3.82) 72.69 (2.66)	-0.32 (0.49) *-0.31 [-0.74- -0.02]* -0.08 (0.52) *0.03 [-0.51-0.29]* -0.46 (0.38) *-0.60 [-0.76- -0.27]*	1684 (153) 1542 (109) 1638 (123)	2.30 (1.12) *2.41 [1.66-2.75]* 1.09 (1.07) *1.09 [0.44-2.07]* 1.67 (1.03) *1.58 [0.87-2.36]*
p-value		p=0.190[2]		p=0.085[2]		p<0.05[2] Post-hoc non-significant

1. **Kruskal-Wallis rank sum test (post-hoc Conover's test, Bonferroni correction)**
2. ***2.*** **One-way ANOVA (post-hoc pairwise T-test)**

Table 4. Postoperative photocephalometric measurements

Figure 1

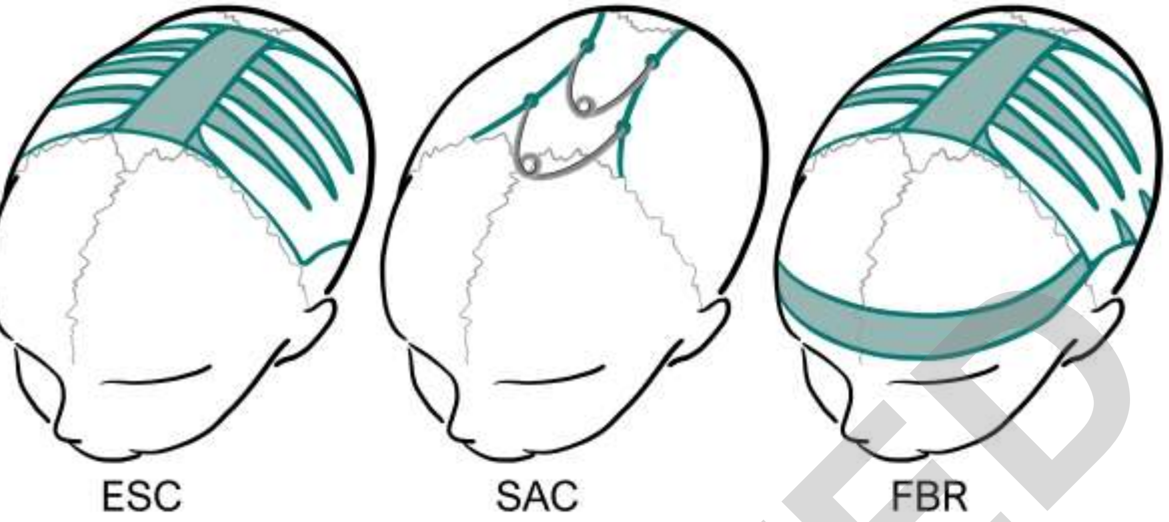

Figure 2

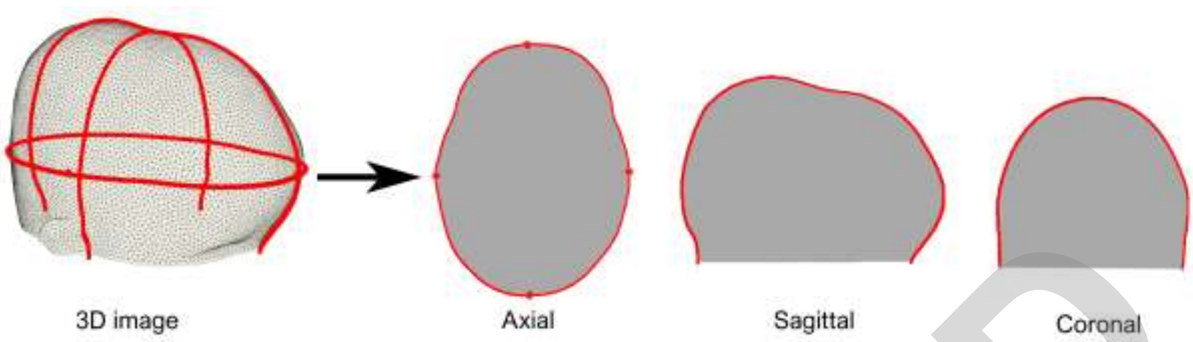

Figure 3

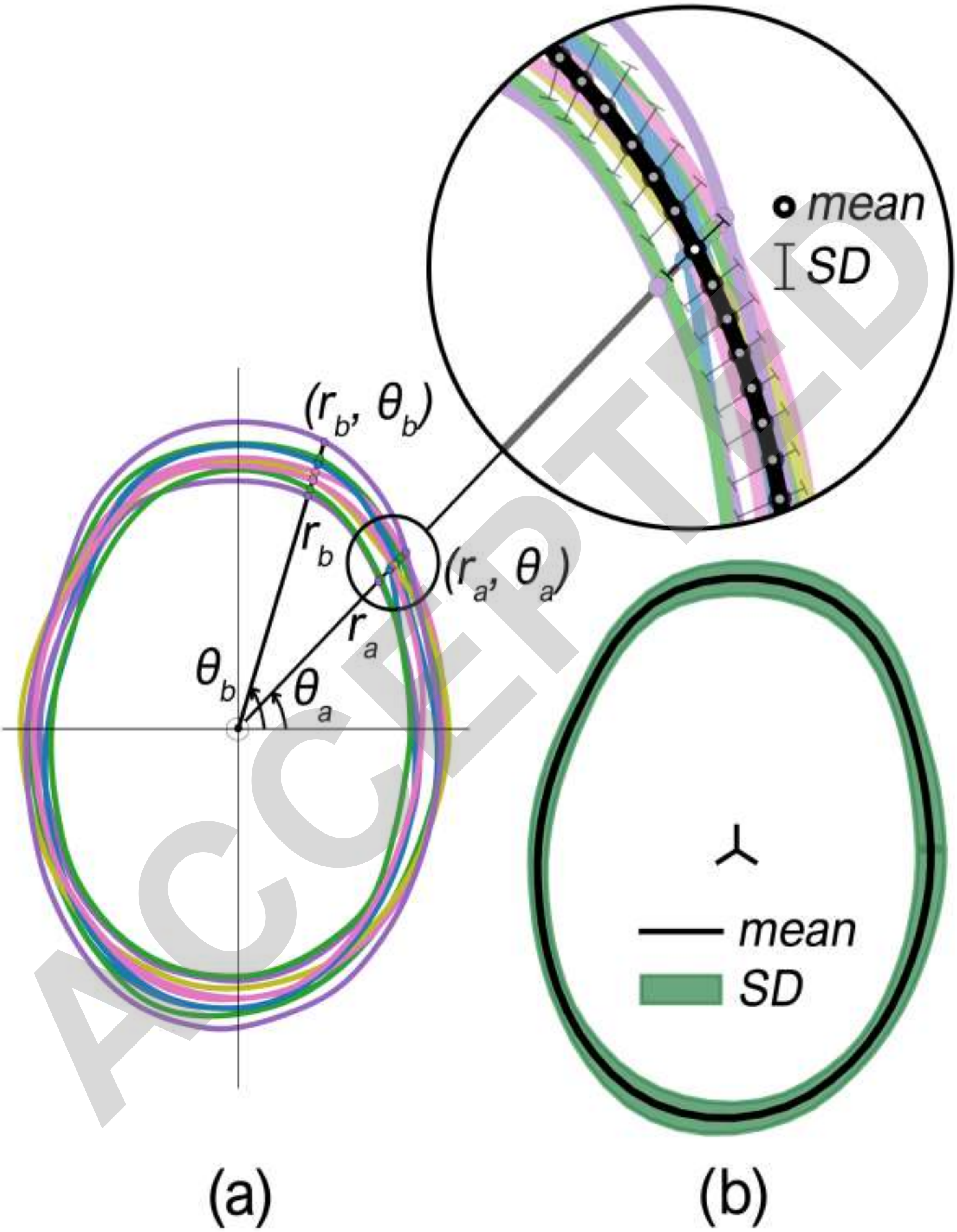

Figure 4

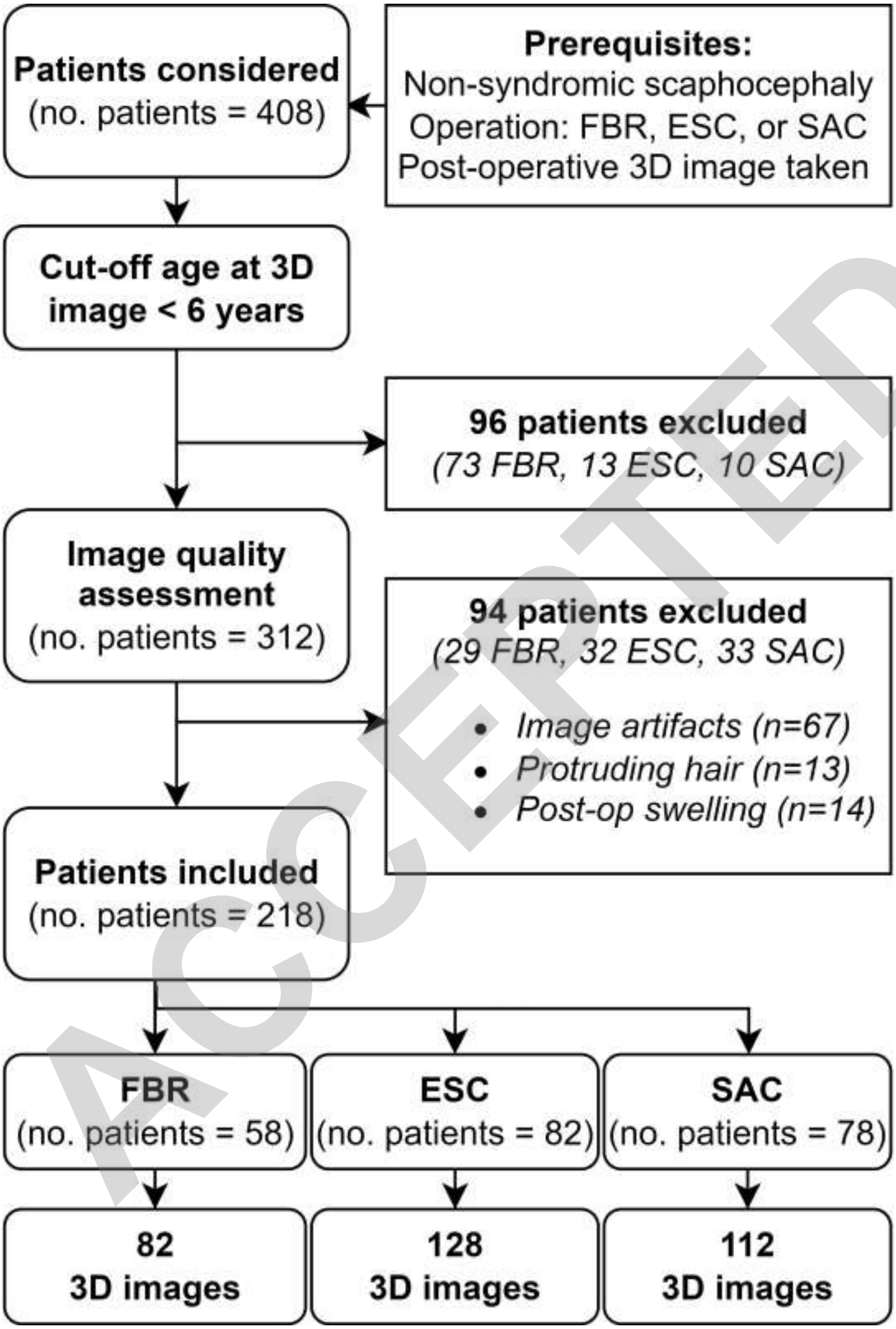

Patients considered
(no. patients = 408)
Prerequisites:
Non-syndromic scaphocephaly
Operation: FBR, ESC, or SAC
Post-operative 3D image taken
Cut-off age at 3D image < 6 years
96 patients excluded
(73 FBR, 13 ESC, 10 SAC)
Image quality assessment
(no. patients = 312)
94 patients excluded
(29 FBR, 32 ESC, 33 SAC)
Image artifacts (n=67)
Protruding hair (n=13)
Post-op swelling (n=14)
Patients included
(no. patients = 218)
FBR
(no. patients = 58)
ESC
(no. patients = 82)
SAC
(no. patients = 78)
82
3D images
128
3D images
112
3D images

Figue 5

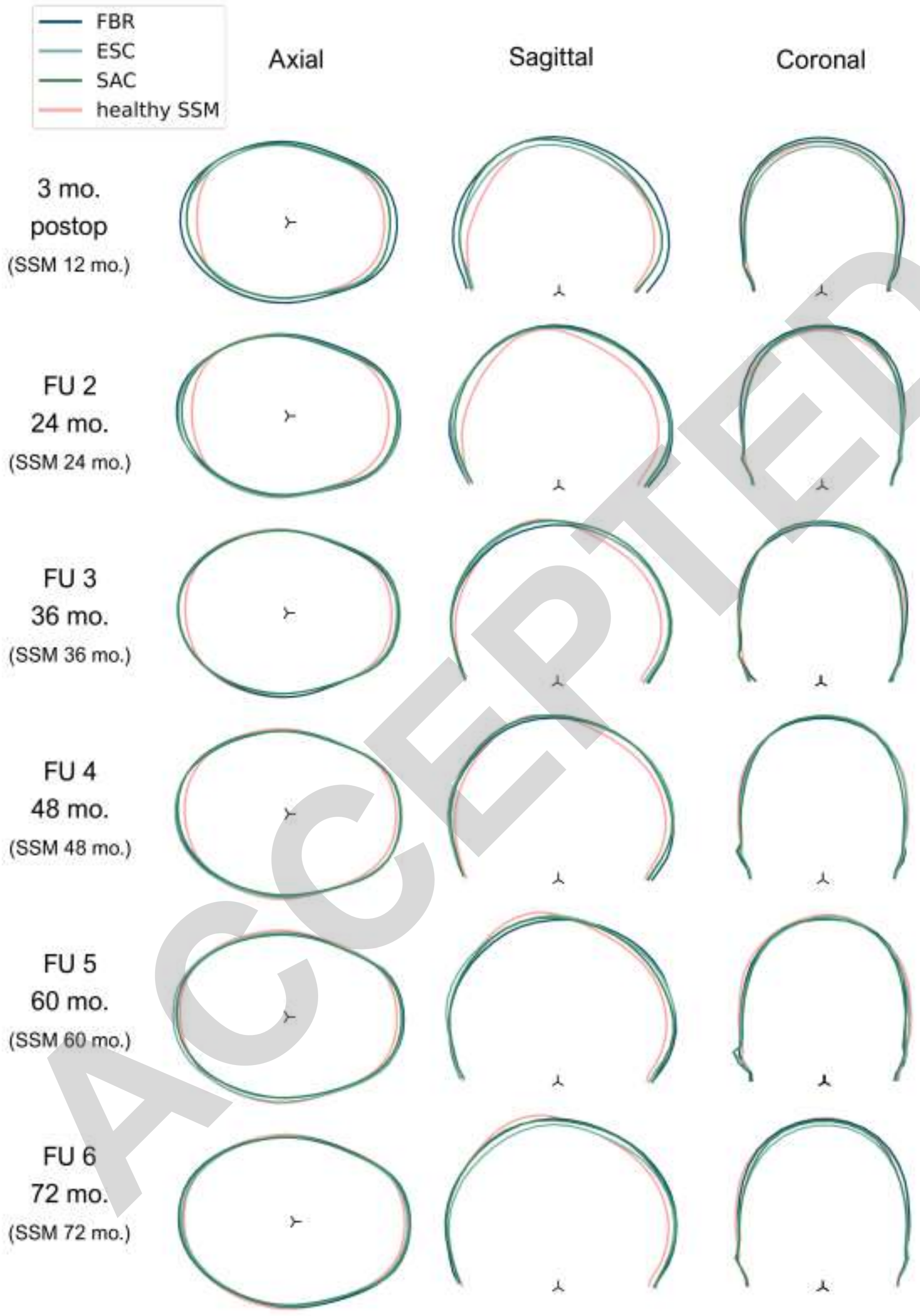
FBR
ESC
SAC
healthy SSM
Axial
Sagittal
Coronal
3 mo.
postop
(SSM 12 mo.)
FU 2
24 mo.
(SSM 24 mo.)
FU 3
36 mo.
(SSM 36 mo.)
FU 4
48 mo.
(SSM 48 mo.)
FU 5
60 mo.
(SSM 60 mo.)
FU 6
72 mo.
(SSM 72 mo.)

Figure 6

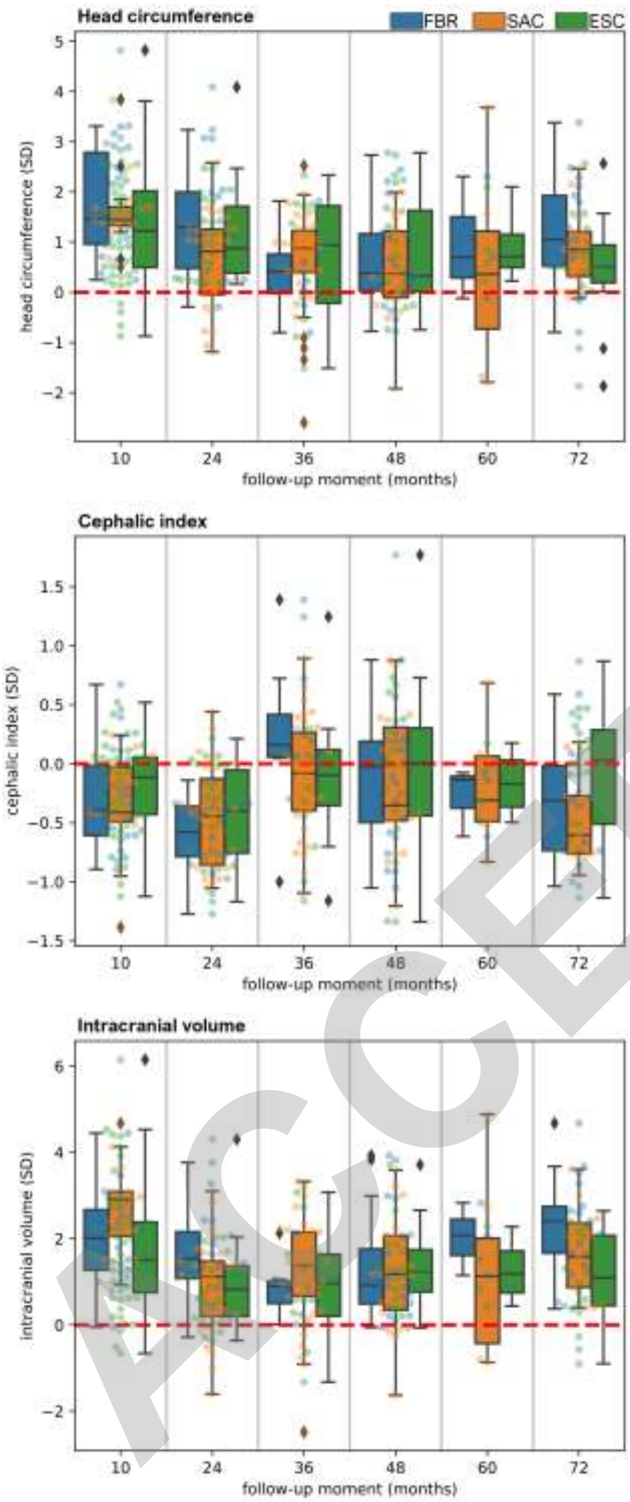

Head circumference
FBR
SAC
ESC
head circumference (SD)
follow-up moment (months)
Cephalic index
cephalic index (SD)
follow-up moment (months)
Intracranial volume
intracranial volume (SD)
follow-up moment (months)

SDC 1

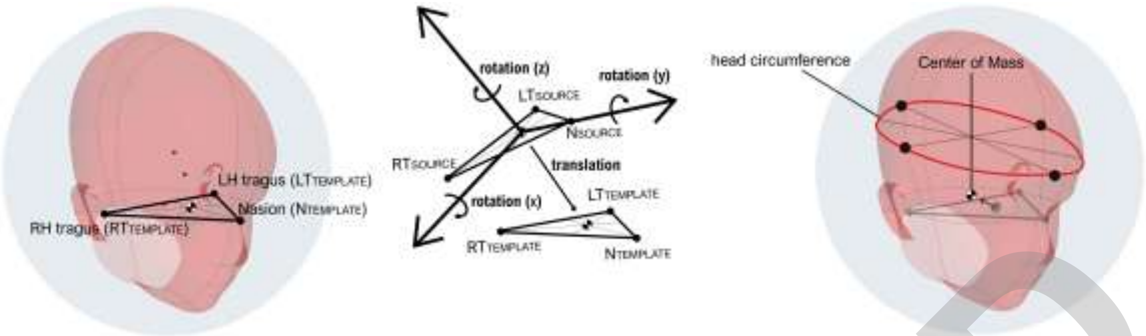
LH tragus (LTTEMPLATE)
Nasion (NTEMPLATE)
RH tragus (RTTEMPLATE)
rotation (z)
rotation (y)
LTSOURCE
NSOURCE
RTSOURCE
translation
rotation (x)
LTTEMPLATE
RTTEMPLATE
NTEMPLATE
head circumference
Center of Mass

Supplemental Digital Content 2

Pre-processing of 3D photogrammetry images

The nasion and both tragi are manually identified, after which meshes are automatically registered to a healthy template from a statistical shape model.[1] For this registration step and further analysis, a standardized reference frame for aligning 3D images is essential. The origin of this reference frame should be defined such that it represents a stable point in the cranium that does not shift during growth. Several reference planes for 3D photogrammetry based on external landmarks have been used in literature.[2–6]

For our study, we selected the nasion-tragi plane as our frame of reference. The centroid of the three landmarks (nasion, left tragus, and right tragus) serves as the initial anchor point and guide the image registration process.

The required translation of the mesh is described by the Euclidian distance between the landmark centroid of the source mesh (i.e. mean [□, □, □] position of the three selected landmarks) and the landmark centroid of the target (template) mesh. Iteratively, the mesh is rotated along each axis until the three vectors are aligned with the corresponding vectors on the template. Because the centroid of the three landmarks is not a direct function of the posterior region, the center of mass was extracted from the head circumference slice. The discrepancy between the initial centroid and the center of mass was calculated, and finally a translation was applied to the mesh (in anterior-posterior direction). This translated centroid is located at the origin of the frame of reference ([□, □, □] = [0,0,0]).

The shape and number of mesh elements influence the accuracy of the 3D representation. For comparative analysis, resampling of the meshes is performed to model each 3D image with the same number of uniformly distributed triangular elements using Voronoi clustering implemented in the *pyacvd* library.[7] Mesh interaction was mainly based on the PyVista library.[8] Small mesh defects are automatically repaired using an iterative repair algorithm that can detect and remove undesired elements, returning a water tight model.[9]

1. T. Huysmans, L. Goto, J. Molenbroek RG. DINED Mannequin. *Tijdschr voor Hum Factors*. 2020;45(1):4--7.

2. McKay DR, Davidge KM, Williams SK, et al. Measuring cranial vault volume with three-dimensional photography: A method of measurement comparable to the gold standard. *J Craniofac Surg*. 2010;21(5):1419-1422.

doi:10.1097/SCS.0b013e3181ebe92a

3. Seeberger R, Hoffmann J, Freudlsperger C, et al. Intracranial volume (ICV) in isolated sagittal craniosynostosis measured by 3D photocephalometry: A new perspective on a controversial issue. *J Cranio-Maxillofacial Surg*. 2016;44(5):626-631. doi:10.1016/j.jcms.2016.01.023

4. Martini M, Klausing A, Lüchters G, Heim N, Messing-Jünger M. Head circumference - a useful single parameter for skull volume development in cranial growth analysis? *Head Face Med*. 2018;14(1):3. doi:10.1186/s13005-017-0159-8

5. Weinberg SM, Naidoo S, Govier DP, Martin RA, Kane AA, Marazita ML. Anthropometric precision and accuracy of digital three-dimensional photogrammetry: Comparing the genex and 3dMD imaging systems with one another and with direct anthropometry. *J Craniofac Surg*. 2006;17(3):477-483. doi:10.1097/00001665-200605000-00015

6. Schaaf H, Pons-Kuehnemann J, Malik CY, et al. Accuracy of three-dimensional photogrammetric images in non-synostotic cranial deformities. *Neuropediatrics*. 2010;41(1):24-29. doi:10.1055/s-0030-1255060

7. pyacvd. https://github.com/pyvista/pyacvd

8. Sullivan CB, Kaszynski A. PyVista: 3D plotting and mesh analysis through a streamlined interface for the Visualization Toolkit (VTK). *J Open Source Softw*. 2019;4(37):1450. doi:10.21105/joss.01450

9. Attene M. A lightweight approach to repairing digitized polygon meshes. *Vis Comput*. 2010;26(11):1393-1406. doi:10.1007/s00371-010-0416-3

Follow-up group **No. of samples**	**Shapiro-Wilk test** **P > 0.05:** **Gaussian distribution** **|FBR|ESC|SAC|**	**Levene's test** **P > 0.05:** **Equal variance**	**One-way Anova**	**Kruskal-Wallis test**
FU1	**OFC** |0.128|0.489|0.033|	0.180		X
3 months postop	**CI** |0.322|0.415|0.275|	0.752	X	
FBR: 18, ESC: 48, SAC: 13	**ICV** |0.984|0.053|0.974|	0.495	X	
FU2	**OFC** |0.440|0.033|0.419|	0.665		X
24 months	**CI** |0.456|0.378|0.188|	0.501	X	
FBR: 16, ESC: 26, SAC: 26	**ICV** |0.985|0.006|0.821|	0.677		X
FU3	**OFC** |0.994|0.137|0.013|	0.418		X
36 months	**CI** |0.430|0.153|0.991|	0.859	X	
FBR: 8, ESC: 11, SAC: 34	**ICV** |0.386|0.950|0.348|	0.217	X	
FU4	**OFC** |0.144|0.059|0.620|	0.815	X	
48 months	**CI** |0.711|0.570|0.125|	0.564	X	
FBR: 20, ESC: 21, SAC: 17	**ICV** |0.006|0.279|0.956|	0.286		X
FU5	**OFC** |0.651|0.375|0.681|	0.506	X	
60 months	**CI** |0.196|0.803|0.980|	0.475	X	
FBR: 3, ESC: 4, SAC: 9	**ICV** |0.892|0.853|0.454|	0.345	X	
FU6	**OFC** |0.973|0.225|0.475|	0.552	X	
72 months	**CI** |0.710|0.639|0.105|	0.603	X	
FBR: 17, ESC: 18, SAC: 13	**ICV** |0.958|0.489|0.570|	0.952	X	

Table, SDC 3. Statistical test selection for continuous variables

	FBR (n=58)	ESC (n=82)	SAC (n=78)	Overall (n=218)
ICH	1 (2.0%)	4 (5.4%)	1 (1.4%)	6 (3.1%)
Re-intervention	5 (8.6%)	8 (9.6%)	2 (2.6%)	15 (6.8%)
ICH	1	3	1	5
Skull defect	4	3	-	7
Persisting scaphocephalic shape	-	1	1	2
Hematoma	-	1	-	1

Table, SDC 4. ICH and re-interventions

	FBR	ESC	SAC	Overall	p-value
No. of measurements [1]	31	61	57	149	
OFC (cm) Mean (SD)	47.43 (2.17)	42.81 (2.13)	43.04 (1.93)	43.86 (2.75)	
OFC (z-score) Mean (SD) Median [IQR]	2.10 (1.77) 2.14 [0.92-2.87]	1.65 (1.32) 1.95 [0.88-2.38]	1.92 (0.94) 1.95 [1.18-2.52]	1.85 (1.31) 1.95 [1.06-2.52]	0.501 [3]
No. of measurements [2]	12	32	15	59	
CI (%) Mean (SD)	66.52 (3.93)	66.17 (3.59)	67.45 (3.01)	66.57 (3.51)	
CI (z-score) Mean (SD) Median [IQR]	-1.49 (0.55) -1.45 [-1.86- -1.12]	-1.38 (0.53) -1.50 [-1.78- -0.90]	-1.25 (0.32) -1.23 [-1.45- -1.14]	-1.36 (0.49) -1.36 [-1.76- -1.07]	0.469 [4]

1. **Measurements obtained in clinic (measuring tape)**
2. **Measurements obtained from preoperative skull radiographs**
3. **Kruskal-Wallis rank sum test**
4. **One-way ANOVA**

Table, SDC 5. Preoperative baseline evaluation

SDC 6

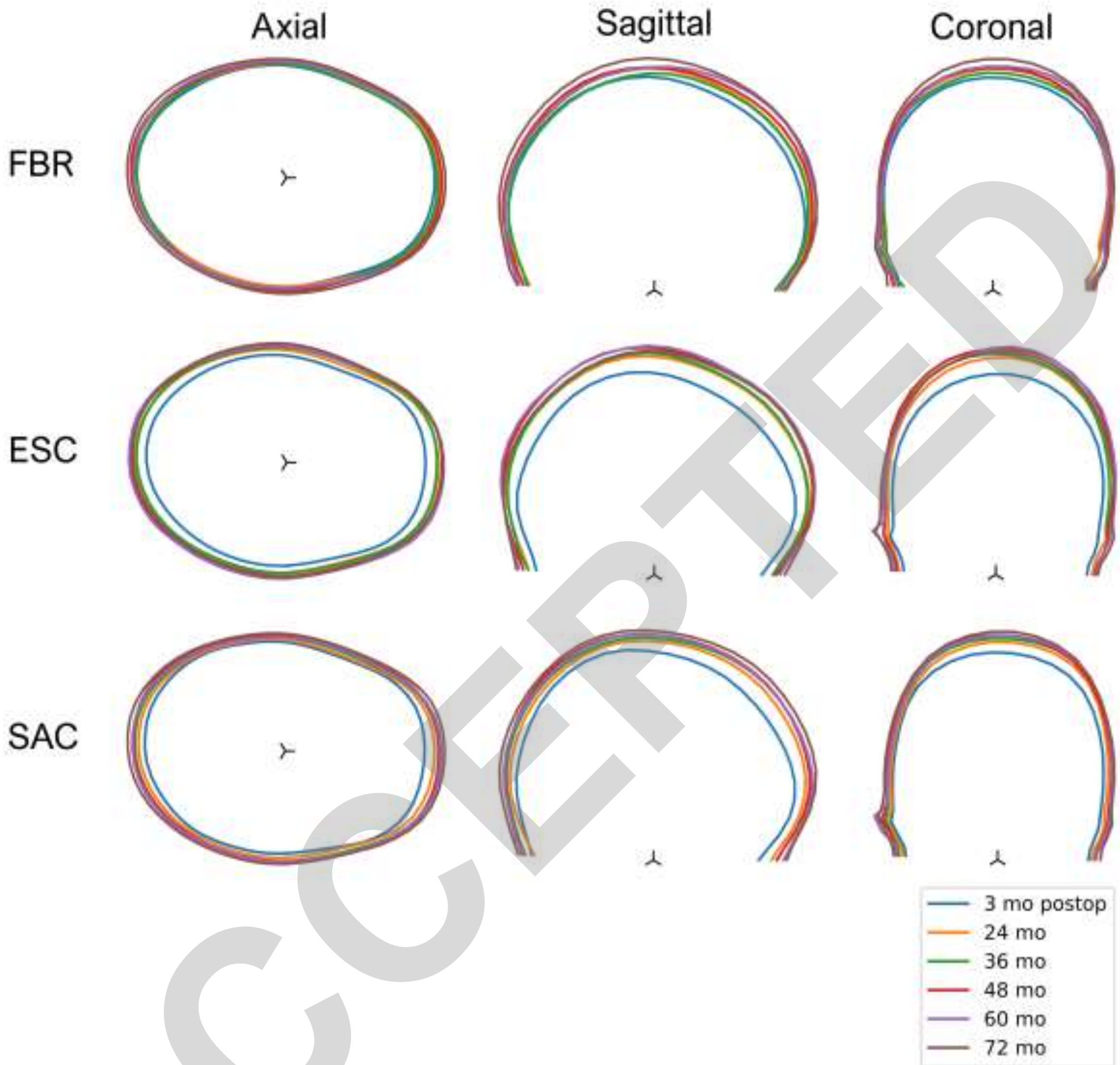
Axial
Sagittal
Coronal
FBR
ESC
SAC
3 mo postop
24 mo
36 mo
48 mo
60 mo
72 mo